JOINT INSTITUTE FOR NUCLEAR RESEARCH

Veksler and Baldin laboratory of High Energy Physics

FINAL REPORT ON THE SUMMER STUDENT PROGRAM

Investigation of strongly interacting matter produced at energies of beam energy scan program at STAR

Supervisor: Alexey Aparin, JINR

Student: Nikolskaia Larisa Andreevna, Russia

Ufa State Aviation Technical University

Participation Period: June 30 - August 25

Dubna, 2018

Abstract

This work presents the results that was obtained during summer practice in the laboratory of high energy physics. The main goal of the work was to investigate the process of phase transition in hot and dense nuclear matter. Existence of the phase transition was confirmed in heavy ion collisions at Relativistic Heavy Ion Collider (RHIC) at energies of 200 GeV. In present work we tried to reproduce one of the specific signatures of phase transition, namely the ratio of strange particle e.g. kaons ($K^{\pm}$), yeilds to non-strange particles e.g. pions ($\pi^{\pm}$) in dependence of the center-of-mass energy.

Contents

1 Introduction

A major goal of high-energy nuclear collisions is to determine the phase diagram for matter that interacts via the strong nuclear force. In contrast to the countless, very distinct phase diagrams found in condensed matter physics, the phase diagram probed in heavy-ion collisions is a unique and fundamental feature of Quantum Chromodynamics (QCD). The most experimentally accessible way to characterize the QCD phase diagram is in the plane of temperature (T) and the baryon chemical potential (μ_B) [4]. Figure 1 shows a schematic layout of the QCD phases, along with hypothesized indications of the regions crossed in the early stages of nuclear collisions at various beam energies.

Hadronic matter is a state in which the fundamental constituents, quarks and gluons, are confined in composite particles, namely baryons and mesons. At high energy densities, QCD predicts a phase transition from a hadronic gas (HG) to a state of deconfined, partonic matter called the quark-gluon plasma (QGP). In hot and dense QCD matter, the hadrons are melted into their constituent quarks, and the strong interaction becomes the dominant feature of the physics.

In order to study experimentally the QCD phase structure as a function of T and μ_B, a scan over beam energies is employed. Several collision energies are used to create systems which form at a variety of initial coordinates in T and μ_B. As the systems evolve, the adiabatic expansion is governed by the QGP equation of state. Therefore, as the system expands, T is reduced and μ_B, which is a measure of the excess of quarks relative to antiquarks, may also evolve. The excess of quarks is due to the valence quarks of the stopped participant baryons from the two colliding nuclei. By creating systems with a broad range of initial conditions, it is hoped that the different reaction trajectories cross the phase boundary at different T and μ_B values and that this allows us to access interesting features in the phase diagram (i.e. critical point and first-order phase transition).

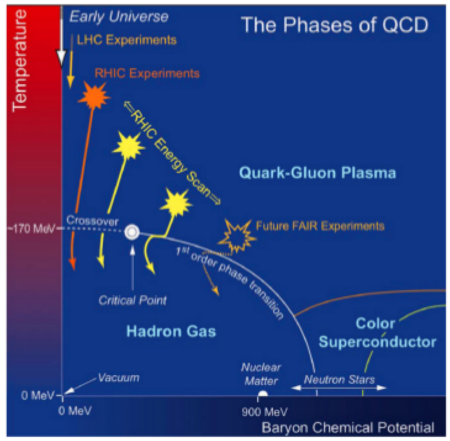

Figure 1: A conjectured QCD phase diagram with boundaries that define various states of QCD matter.

The purpose of the BES-I program was three-fold: (a) to search for threshold energies for the QGP signatures that have already been established at the top RHIC energies, thereby corroborating the past QGP discoveries; (b) to search for signatures of a first-order phase transition; and (c) to search for a QGP/HG critical point. The details of the BES-I program are listed in Figure 2.

Strangeness production has a special place in the physics of heavy-ion collisions. Enhanced production of strangeness has long been predicted as a prominent signature of QGP formation. In a hadron gas strangeness has to be produced via strange hadron pairs which require a large energy, while in QGP it can be produced via a strange quark-antiquark pair, which is energetically favored. Therefore the K/π ratio on the framework of heavy ion collisions is studied in the search QGP formation strangeness productions, trying to find peak on the K^+/π^+ ratio referred what can be related with the phase-transition between hadrons and the QGP. Existence of such a peak is

Beam Energy (in GeV)	Baryon Chemical Potential (in MeV)	Year of Data Taking	Event Statistics (Millions)	Beam Time (Weeks)
200	20	2010	350	11
62.4	70	2010	67	1.5
39	115	2010	130	2.0
27	155	2011	70	1.0
19.6	205	2011	36	1.5
14.5	260	2014	20	3.0
11.5	315	2010	12	2.0
7.7	420	2010	4	4.0

Figure 2: An overview of Beam Energy Scan Phase-I.

Experimentally, different regions of the phase diagram are accessed by changing the beam energy. Both initial T and μ_B vary as functions of the center-of-mass energy $\sqrt{s_{NN}}$. This is the strategy adopted in the BES program at RHIC. It is possible to estimate the T and μ_B regions of the phase diagram accessed for a given collision energy through the study of the hadron spectra. These spectra reflect the properties of the bulk matter at kinetic freeze-out, after elastic collisions among the hadrons have ceased. As an example, Figure 3 shows a representative plot of the invariant yields.

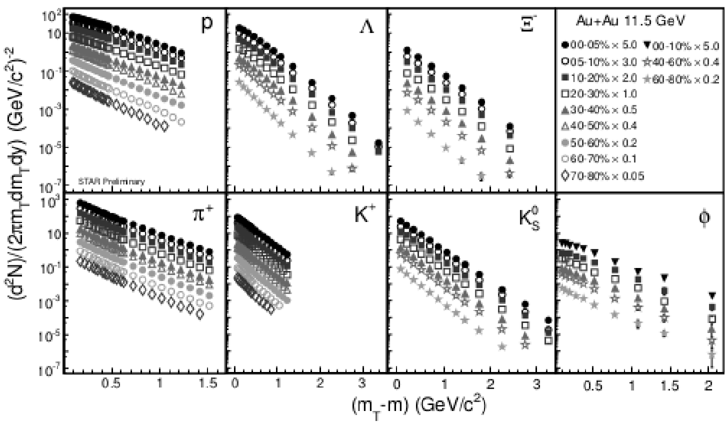

Figure 3: Invariant yields versus m_T - m of hadrons produced in Au+Au collisions at various collision centralities at $\sqrt{s_{NN}} = 11.5$ GeV.

2 STAR experiment

The BES-I program provided measurements of the centrality dependence of the freeze-out parameters. In BES Phase-II, a systematic measurement of the yields of a variety of produced hadrons versus rapidity, centrality, and beam energy will address questions about the evolution of the hadron yields between the initial hadronization and the final thermal equilibrium and about the possibility of successive hadronization.

The RHIC BES-I program scanned from energies for which the matter expands and cools through a crossover transition down to those which could contain key features of the phase diagram of QCD matter, specifically, the detailed study of the energy range from 7.7 to 19.6 GeV proposed in BES Phase-II is well suited to identify the critical point and the first-order phase transition boundary.

Thermodynamic principles suggest that there should be a critical point in QCD matter where the first-order phase transition ends and the transition becomes a crossover, at which point the phase boundaries effectively cease to exist [4].

STAR is one of the major experiments at the Relativistic Heavy-Ion Collider (RHIC) at the Brookhaven National Laboratory, Upton, New York. Its goal is to study the structure of matter with high-energy collisions including polarized p+p collisions for spin physics, d+Au, Cu+Cu and Au+Au collisions for the physics of QGP.

The STAR detector specializes in tracking the thousands of particles produced by each ion collision at RHIC. Weighing 1,200 tons and as large as a house, STAR is a massive detector. It is used to search for signatures of the form of matter that RHIC was designed to create, the quark-gluon plasma.

Detecting and understanding the QGP allows to understand better the universe in the moments after the Big Bang, where the symmetries (and lack of symmetries) of surroundings were put into motion. Unlike some physics experiments where a theoretical idea can be tested directly by a single measurement, STAR must make use of a variety of simultaneous studies in order to draw strong conclusions about the QGP. This is due both to the complexity of the system formed in high-energy nuclear collisions and the unexplored landscape of the physics being studied [7].

STAR therefore consists of several types of detectors, each specializing in detecting certain types of particles or characterizing their motion. These detectors work together in an advanced data acquisition and subsequent physics analysis that allows definitive statements to be made about the collision.

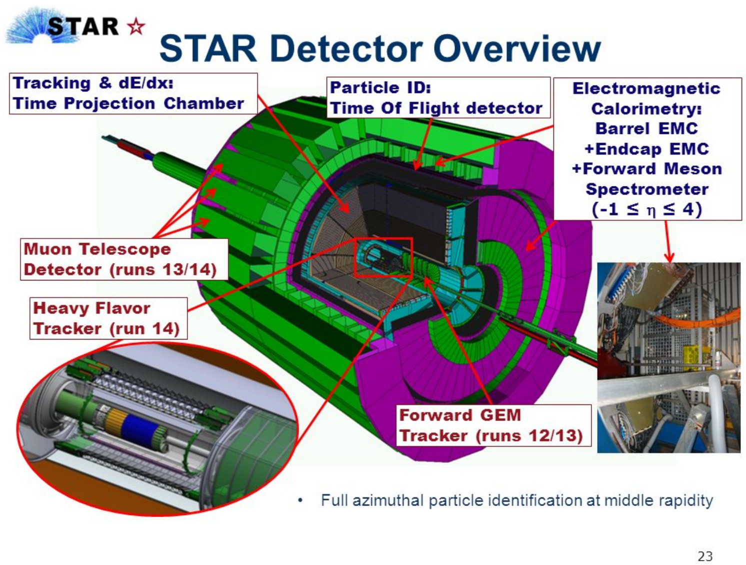

Figure 4: STAR detector.

3 Monte-Carlo models

3.1 THERMINATOR model

THERMINATOR, the THERMal heavy IoN generATOR, created to carry out the statistical hadronization in relativistic heavy-ion collisions.

THERMINATOR 2 is a Monte Carlo generator written in C++ and using the standard CERN ROOT environment. That way, apart from model applications, the code can be easily adapted for purposes directly linked to experimental data analysis, detector modeling, or estimates for the heavy-ion experiments at RHIC, LHC, SPS, FAIR, or NICA.

The code has evolved into a versatile tool, where the freeze-out profile and the expansion velocity field of any shape can be implemented, allowing application to all approaches based on statistical hadronization on a specified hypersurface.

With few physical input parameters, such as the temperature, chemical potentials, size, and the velocity of the collective flow, the models describe the observed particle abundances [1].

The THERMINATOR model was used to generate events in the indicated center-of-mass energy range using the temperature and baryon chemical potential μ_B as input parameters. For this, a table 5 was used for the correspondence of these parameters to a specific center-of-mass energy value, obtained experimentally by researchers.

The particle yields are found to be described, with remarkable precision, by a thermal-statistical model that assumes approximate chemical equilibrium. For a given collision energy, the thermal-statistical model with only two parameters, the temperature (T) and baryon chemical potential (μ_B), provides a very systematic description of particle yields. With increasing collision energy, there is an increase of the chemical freeze-out temperature, T, and a corresponding decrease of the baryon chemical potential, μ_B [2].

Collision System and Energy	Ref.	T (MeV)	μ_B (MeV)	Include in Fits
RHIC				
Au+Au $\sqrt{s} = 200$ AGeV	[6]	177±7	29±6	
	[13]	163±4	24±4	
	[15]	165.6±4.5	28.5±3.7	
Au+Au $\sqrt{s} = 130$ AGeV	[5]	169±6	38.1±4.2	✓
	[6]	174±7	46±5	✓
	[14]	165±7	41±5	✓
SPS				
Pb+Pb 158AGeV $\sqrt{s} = 17.3$ AGeV	[7]	157.5±2.2	248.9±8.2	✓
	[7]	154.6±2.7	245.9±10.0	✓
	[11]	161.0±6.0	260.0±30	✓
Pb+Pb 80AGeV $\sqrt{s} = 12.3$ AGeV	[7]	153.5±4.1	298.2±9.6	✓
	[7]	149.9±5.1	293.8±11.0	✓
	[12]	155.0±5.0	284.0±15.0	✓
Pb+Pb 40AGeV $\sqrt{s} = 8.77$ AGeV	[7]	146.1±3.0	382.4±9.1	✓
	[7]	143.0±3.1	380.8±8.9	✓
	[12]	148.0±5.0	367.0±14.0	✓
Pb+Pb 30AGeV $\sqrt{s} = 7.62$ AGeV	[7]	140.1±3.3	413.7±16.3	✓
	[7]	144.3±4.7	406.0±19.1	✓
Pb+Pb 20AGeV $\sqrt{s} = 6.27$ AGeV	[7]	131.3±4.5	466.7±12.9	✓
	[7]	135.8±5.2	472.5±13.7	✓
AGS				
Au+Au 11.6AGeV $\sqrt{s} = 4.86$ AGeV	[7]	118.7±3.1	554.4±13.0	✓
	[7]	119.2±5.3	578.8±15.4	✓
	[12]	123.0±5.0	558.0±15.0	✓
SIS				
Au+Au 1.0AGeV $\sqrt{s} = 2.32$ AGeV	[8]	52±1.5	822	✓
	[9]	49.6±1	810±15	✓
	[9]	49.7±1.1	818±15	✓
	[10]	58±4	792±7	✓
Au+Au 0.8AGeV $\sqrt{s} = 2.24$ AGeV	[10]	54±2	808±5	✓

Figure 5: Results obtained in statistical-thermal model fits to Au+Au and Pb+Pb collision systems by numerous groups over a wide range of energies

The temperature T and the baryon chemical potential μ_B are shown in Figure 6 as a function of the beam energy. It provides a good quantitative description of the corresponding thermal model results.

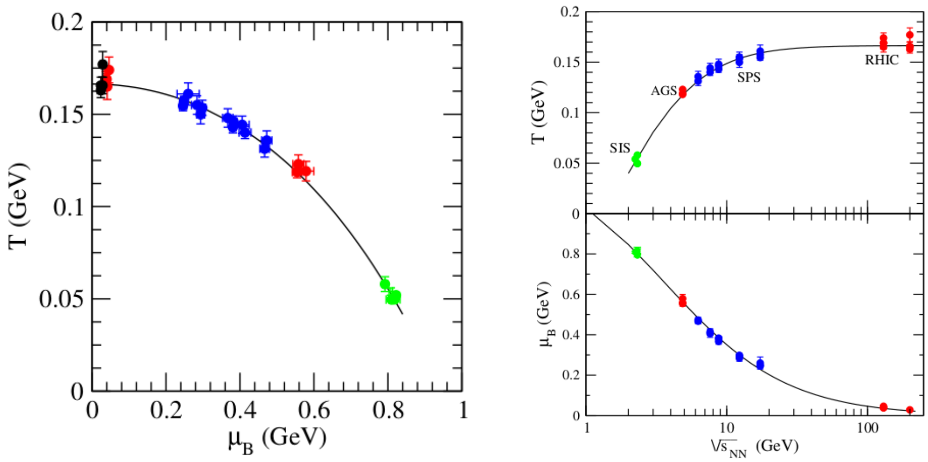

Figure 6: Values of μ_B and T for different energies; Energy dependence of the chemical freeze-out parameters T and μ_B.

So `THERMINATOR 2` was used in our work to generate events.

3.2 UrQMD mode

The Ultrarelativistic Quantum Molecular Dynamics model is a microscopic model used to simulate (ultra)relativistic heavy ion collisions in the energy range from Bevalac and SIS up to AGS, SPS and RHIC, is a fully integrated Monte Carlo simulation package for Proton+Proton, Proton+nucleus and nucleus+nucleus interactions.

The UrQMD model was used to generate the events of the same center-of-mass energy range. For the UrQMD model, the input data is the number of events and center-of-mass energy, which is very convenient for this project. The output data is similar to the output of the `THERMINATOR`, so one can compare the results obtained in different models.

It was used to generate statistics for AuAu collisions so that the ratios of K^+/π^+ and K^-/π^- could be calculated and compared to the results obtained with `THERMINATOR 2`. It is important to say that UrQMD model doesn't have a phase transition mechanism, therefore the results expected with this model and from `THERMINATOR 2` are different.

More information on the results of UrQMD simulation results for this study can be found at the report of other summer practice participant Betania Camille Tumelero Backes.

4 Simulation results

Fifty thousand events were generated for each center-of-mass energy value by `THERMINATOR 2` package using Freeze-out models Lhyquid 2D boost-invariant.

The events were generated at different values of center-of-mass energy, using respective the baryon chemical potential (μ_B) and temperature (T). For this were used table with results obtained in statistical-thermal model fits to Au+Au and Pb+Pb collision systems by numerous groups over a wide range of energies 5.

4.1 p_T spectra of different particles

Fist of all the histograms of spectra with values of pseudo-fastness are less than 1.0 or 0.5 for kaons and pions were obtained 8.

Also histograms were obtained for another values of center-of-mass energies.

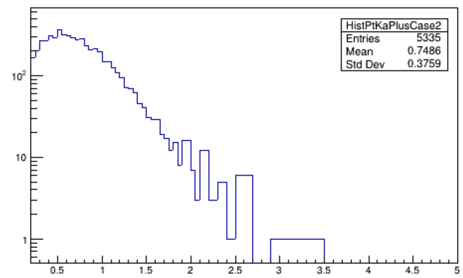

(a) K^+ at $|\eta| \leq 0.5$

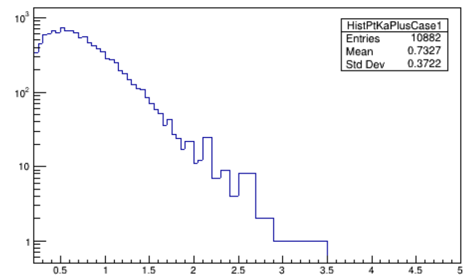

(b) K^+ at $|\eta| \leq 1.0$

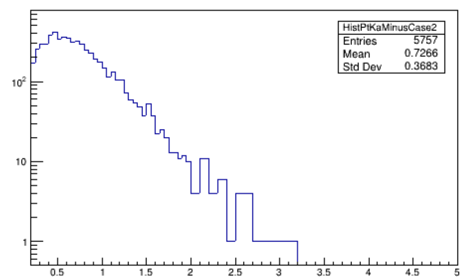

(c) K^- at $|\eta| \leq 0.5$

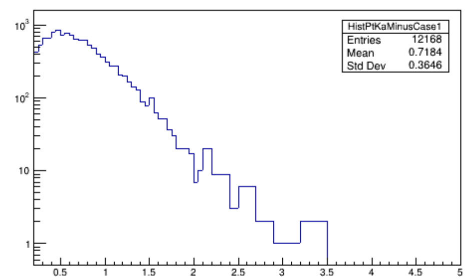

(d) K^- at $|\eta| \leq 1.0$

Figure 7: Histograms of transverse-momentum for Kaons at the energy $\sqrt{s_{NN}} = 7.62$ GeV with cut $p_T \geq 0.2$ and pseudorapidity $|\eta| \leq 0.5$ or $|\eta| \leq 1.0$

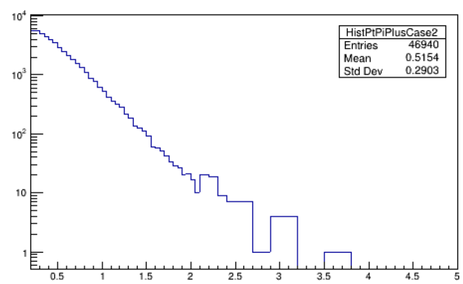

(a) π^+ at $|\eta| \leq 0.5$

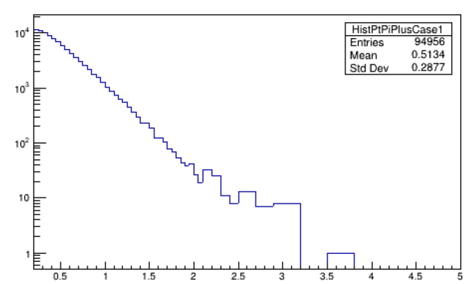

(b) π^+ at $|\eta| \leq 1.0$

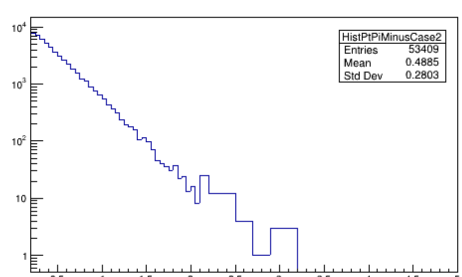

(c) π^- at $|\eta| \leq <0.5$

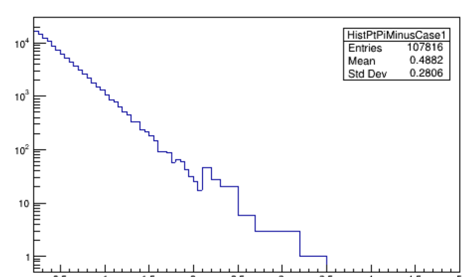

(d) π^- at $|\eta| \leq 1.0$

Figure 8: Histograms of transverse-momentum for Pions at the energy $\sqrt{s_{NN}} = 7.62$ GeV with cut $p_T \geq 0.2$ and pseudorapidity $|\eta| \leq 0.5$ or $|\eta| \leq 1.0$

4.2 K^+/π^+ and K^-/π^- ratios

For each value collision energy, the number of pions and kaons was calculated, and then their ratio. Calculations were carried out under minimal cuts conditions of pseudorapidity $(\eta) < 1.0$ and transverse-momentum $(p_T) > 0.2$. Figure 9 represents the dependence of the kaon and pion ratios of collision energy.

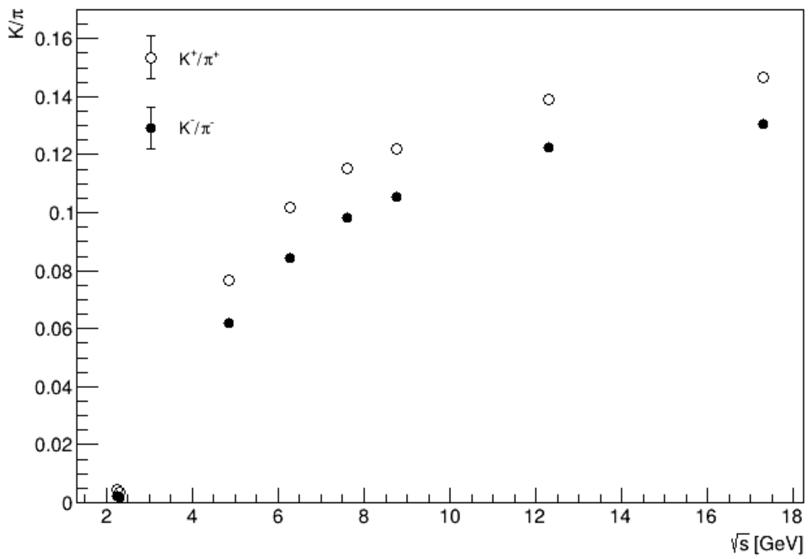

Figure 9: The K^+/π^+ and K^-/π^- ratios as a function of the collision energy in pp and central heavy-ion collisions.

The Figure 9 shows that K^+/π^+ and K^-/π^- ratio in heavy-ion collisions steadily increases with $\sqrt{s_{NN}}$.

Figure 10 compiles the K/π ratios in pp collisions and central heavy-ion collisions as a function of the collision energy $\sqrt{s_{NN}}$. This graph shows which dependence was expected.

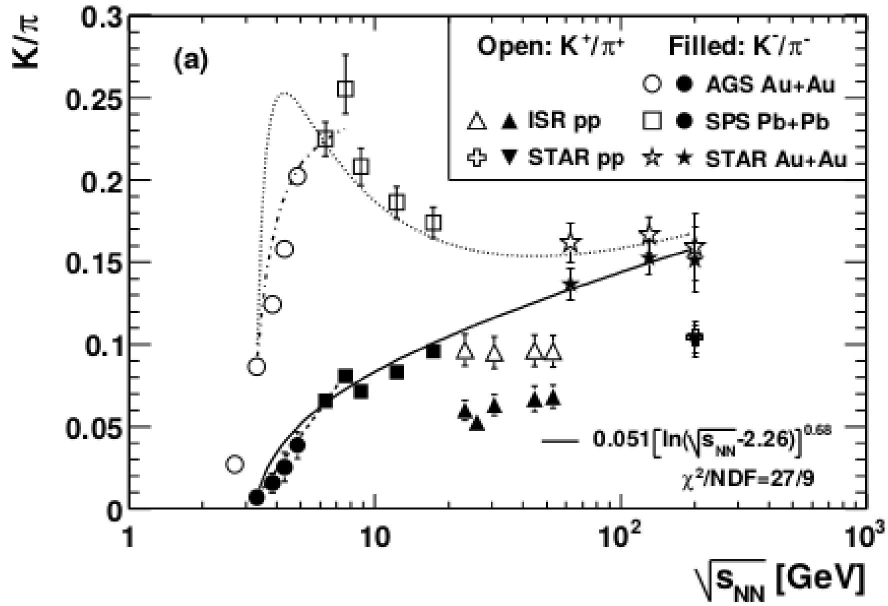

Figure 10: The $K^+/\pi^+ andK^-/\pi^-$ ratios as a function of the collision energy in pp and central heavy-ion collisions by ??? from [7].

In this figure the K^-/π^- ratio in heavy-ion collisions steadily increases with $\sqrt{s_{NN}}$, while K^+/π^+ sharply increases at low energies. The addition of the K^+/π^+ measurements at RHIC energies clearly demonstrates that K^+/π^+ drops at high energies. But there is no such dependence in the received graph [2].

4.3 K^+/K^- ratio

A graph of the ratio of K^+/K^- was also obtained 11. For fitting was used the function in the following form $[p0] \cdot \left[\frac{\ln(\sqrt{s_{NN}}+[p1])}{\ln(\sqrt{s_{NN}}-[p2])}\right]^{1.69}$, where p0, p1, p2 it is automatically selectable parameters. When the fit was applied, the following values of the parameters were obtained:

p0 = 0.901742 ± 0.0256056; p1 = -0.814085 ± 0.577873; p2 = 0.882045 ± 0.476231.

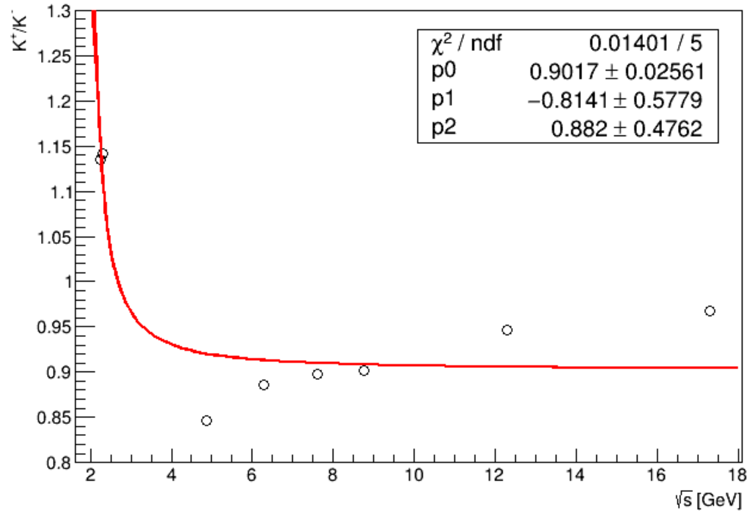

Figure 11: Simulated K^+/K^- ratios as a function of the collision energy in pp and central heavy-ion collisions.

The Figure 12 shows that what function ratio of K^+/K^- were expected to receive. So we got similar results.

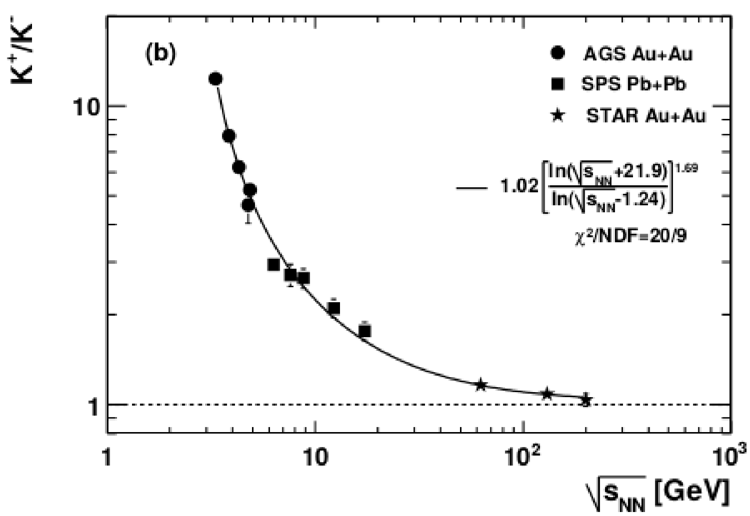

Figure 12: Experimental ratio of K^+/K^- as a function of the collision energy in central heavy-ion collisions from [7]

4.4 π^+/π^- ratio

A graph of the ratio of π^+/π^- was also obtained. So we have an different ratio of π^+/π^-, not like ratio K^+/K^-. The Figure 13 shows that π^+/π^- ratio steadily increases with $\sqrt{s_{NN}}$.

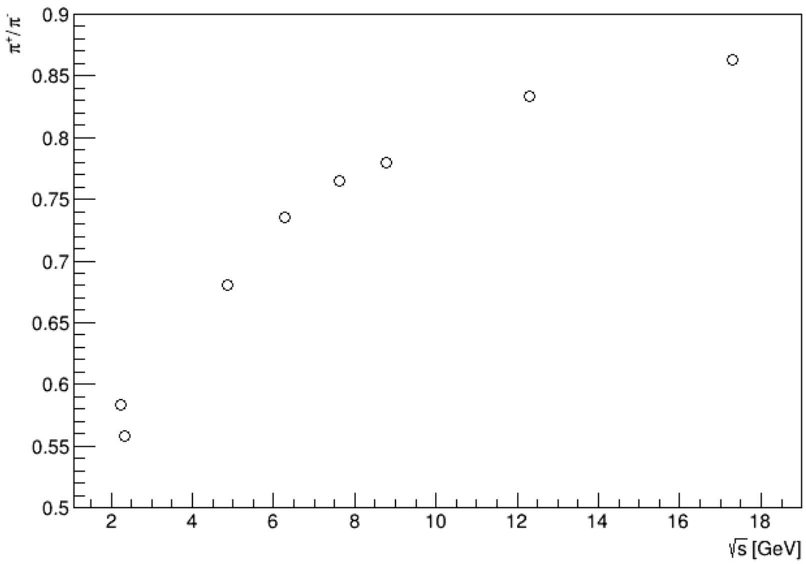

Figure 13: The π^+/π^- ratios as a function of the collision energy in pp and central heavy-ion collisions.

5 Conclusions

Gold-gold collision simulations were performed at the range of center-of-mass energies $\sqrt{s_{NN}} = 2.32$, 4.86, 6.27, 7.62, 8.77, 12.3 and 17.3 GeV. The statistics of fifty thousand events was obtained in the `THERMINATOR` and UrQMD Monte-Carlo generators. The results of the simulation were compared with the experimental ones. The dependences of the ratio K/π on the collision energy were obtained and a comparison was made with the experimental data. For K^+/π^+, it was not possible to obtain the same dependence wich can be a strong evidence of non-applicability of thermodynamical approach to collisions at such energies.

I have improved my skills of working with C++ and learned to work in a new program ROOT and Monte-Carlo generators (UrQMD, `THERMINATOR`). During the work I got a lot of new knowledge in the field of particle physics.

6 Acknowledgements

I want to express my gratitude to the University Center of JINR for giving me the opportunity to participate in the Summer Student Program and Joint Institute for Nuclear Research for providing a financial support.

Also I would like to express my gratitude to Anna Shishkina for her recommendation which allowed me to take part in the program.

I would like to express my gratitude to my supervisor Alexey Aparin, who gave me an excellent opportunity to complete an internship at JINR and provided support throughout the project.

References

[1] M. Chojnacki, A. Kisiel, W. Florkowski, and W. Broniowski, "THERMINATOR 2: THERMal heavyIoN generATOR 2," 2011.

[2] J. Cleymans, H. Oeschler, K. Redlich, and S. Wheaton, "Comparison of Chemical Freeze-Out Criteriain Heavy-Ion Collisions," Phys. Rev., vol. C73, p. 034905, 2005.

[3] B. Abelev et al., “Systematic Measurements of Identified Particle Spectra in pp, d+Au and Au+Au Collisions from STAR,” Phys. Rev., vol. C79, p. 034909, 2009.

[4] ”Studying the Phase Diagram of QCD Matter at RHIC”, 2017.

[5] https://urqmd.org/documentation

[6] https://root.cern.ch/

[7] https://www.bnl.gov/rhic/STAR.asp

[8] http://www.star.bnl.gov/